THE INFLUENCE OF SEISMIC WAVELET PHASE ON REFLECTION COEFFICIENT INVERSION RESULTS

YANAN ZHANG, YONGSHOU DAI, JINJIE DING, MANMAN ZHANG and RONGRONG WANG

College of Information and Control Engineering, China University of Petroleum, Dongying 257061, P.R. China. ufo995-ufo@163.com

(Received September 7, 2013; revised version accepted February 21, 2014)

ABSTRACT

Zhang, Y., Dai, Y., Ding, J., Zhang, M. and Wang, R., 2014. The influence of seismic wavelet phase on reflection coefficient inversion results. *Journal of Seismic Exploration*, 23: 131-152.

To research the influence of seismic wavelet phase on reflection coefficient inversion, an Autoregressive Moving Average (ARMA) model was used to describe the seismic wavelet, the wavelets with the same amplitude spectrum and different phase spectra were constructed by symmetrical mapping Pole-Zeros of the ARMA model in the z-domain, and spectrum division was used to implement reflection coefficient inversion. The theoretical analysis shows that a phase-only filter was remained after reflection coefficient inversion in the condition of inaccurate seismic wavelet phase estimation, and the phase spectrum of the phase-only filter was the phase spectrum difference between real wavelet and constructed wavelet. The real or accurate reflection coefficient sequences were identified in inversion results by the evaluation methods of Kurtosis and Variation. Simulation and actual seismic data processing results also verified the law of the wavelet phase influence on reflection coefficient inversion and the effectiveness of the evaluation methods. Research interest for enhancing the precision of reflection coefficient inversion results was indicated.

KEY WORDS: seismic wavelet, reflection coefficient inversion, phase-only filter, kurtosis, variation.

0963-0651/14/$5.00

INTRODUCTION

Seismic wavelet estimation is an important component of seismic data processing and seismic interpretation. But the wavelet phase is not always estimated accurately in wavelet estimation process, it affects seismic inversion and seismic interpretation. In view of the problem of accurate wavelet phase extraction, some related scholars did a lot of research. Tang divided the wavelet phase into the maximum part and the minimum part, recovered them by Higher-order cumulent methods and estimated the wavelet phase (Tang and Yin, 2001). Yi constructed mixed phase filter by using delay factor and implemented mixed phase deconvolution, the deconvolution results were constrained by minimum entropy criterion and norm, then the optimum filter and wavelet phase were obtained (Yi and Wang, 2006). Cui estimated wavelet amplitude by seismic trace autocorrelation, estimated wavelet phase through the bispectrum method, and constructed mixed phase seismic wavelet finally (Cui and Rui, 2011). But in practice, the above methods are difficult to get the accurate wavelet phase and may cause the distortion of inversion results. In order to improve the inversion results, researchers at home and abroad proposed various phase correction methods. Levy assumed that the difference of estimated wavelet and real wavelet is a constant which is not dependent on frequency, the constant phase correction method was used to correct inversion results in order to eliminate the influence of inaccurate wavelet phase estimation (Levy and Oldenburg, 1982, 1987). Wang proposed a constant Q inverse filtering method based on wavefield continuation theory, and corrected the amplitude and phase of earth Q filtering by using two exponential terms (Wang, 2003, 2006). So far, the various phase correction methods did not eliminate the influence of inaccurate wavelet phase estimation completely. The research about the influence of wavelet phase on inversion will be the research topics and hotspot in the future. Under moving average model description, Yuan discussed the influence of inaccurate wavelet phase on inversion results (Yuan, 2011). Because the model contains too many parameters which result in a variety of phase possibility, and the wavelet length is too short, so it has certain difference comparing with the actual wavelet (Liang, 1998). Therefore, on the base of ARMA model, this paper will ignore the effects of noise to discuss the influence of wavelet phase on inversion and research the influencing rules by the theoretical analysis and simulation.

In this paper, the wavelets with the same amplitude spectrum and different phase spectra will be constructed by symmetrical mapping Pole-Zeros of ARMA model in z-domain. We will implement reflection coefficient inversion to synthetic seismogram, and analyze the inversion results. The theoretical analysis results will be verified by simulation experiment and the actual seismic data processing. This paper will evaluate the inversion results with two methods to determine the real or accurate reflection coefficient sequences.

STRUCTURE OF SEISMIC WAVELETS WITH DIFFERENT PHASE

Spectra

Dai estimated the wavelet with the ARMA model. Relative to the MA model, the ARMA model has the parameter parsimonious characteristic (Dai and Wang, 2008). It can describe an accurate wavelet with less parameters. ARMA model of the filter system is showed as follows,

$$\sum_{i=0}^{p} a_i x(n - i) = \sum_{k=0}^{q} b_k r(n - k) \quad , \tag{1}$$

where x(n) is the seismic record, r(n) is reflection coefficient sequences. AR parameters a_i and MA parameter b_k are real numbers, p is AR order, q is MA order.

The wavelet system function of the ARMA model is assumed to be free of pole-zero cancellations, and is given by

$$W(z) = \sum_{m=0}^{\infty} w(m)z^{-m} = \sum_{k=0}^{q} b_k z^{-k} / \sum_{i=0}^{p} a_i z^{-i}$$

$$= A[\prod_{k=1}^{q}(1-c_k z^{-1}) / \prod_{i=1}^{p}(1-d_i z^{-1})] = A[\prod_{k=1}^{q} C_k(z) / \prod_{i=1}^{p} D_i(z)] \quad , \tag{2}$$

where w(m) is the time-domain sequence of the seismic wavelet, W(z) is its z-domain representation. Because a_i and b_k are real coefficients, system zero c_k and pole d_i are real roots or conjugate complex roots, A is the gain constant.

When $z = e^{j\omega}$, eq. (2) can be converted into the frequency response,

$$W(e^{j\omega}) = A[\prod_{k=1}^{q}(1-c_k e^{-j\omega}) / \prod_{i=1}^{p}(1-d_i e^{-j\omega})] = A[\prod_{k=1}^{q} C_k(e^{j\omega}) / \prod_{i=1}^{p} D_i(e^{j\omega})]$$

$$= A[\prod_{k=1}^{q} C_k(\omega)e^{j\varphi_{Ck}(\omega)} / \prod_{i=1}^{p} D_i(\omega)e^{j\varphi_{Di}(\omega)}] = W(\omega)e^{j\varphi_W(\omega)} \quad , \tag{3}$$

where $j = \sqrt{-1}$ is an imaginary unit, ω is the digital angular frequency. $W(\omega)$ is the amplitude spectrum of the filter, $\varphi_W(\omega)$ is the phase spectrum of the filter. $C_k(\omega)$ and $D_i(\omega)$ are the amplitude spectrum of each component, $\varphi_{Ck}(\omega)$ and $\varphi_{Di}(\omega)$ are the phase spectrum of each component. Where $C_k(e^{j\omega}) = 1 - c_k e^{-j\omega}$, $c_k = x_k + jy_k$,

$$C_k(e^{j\omega}) = 1 - c_k e^{-j\omega} = 1 - (x_k + jy_k)(\cos\omega - j\sin\omega)$$

$$= [1 - x_k\cos\omega - y_k\sin\omega] + j[x_k\sin\omega - y_k\cos\omega]$$

$$= C_k(\omega)e^{j\varphi_{Ck}(\omega)} \quad . \tag{4}$$

The amplitude spectrum $C_k(\omega)$ and phase spectrum $\varphi_{Ck}(\omega)$ of $C_k(e^{j\omega})$ are obtained as,

$$C_k(\omega) = \sqrt{(1 + x_k^2 + y_k^2 - 2x_k\cos\omega - 2y_k\sin\omega)} \quad , \tag{5}$$

$$\varphi_{Ck}(\omega) = \arctan[(x_k\sin\omega - y_k\cos\omega)/(1 - x_k\cos\omega - y_k\sin\omega)] \quad . \tag{6}$$

In a similar way, when $d_i = s_i + jl_i$, we can obtain the amplitude spectrum and phase spectrum of the ARMA model by eqs. (5) and (6),

$$W(\omega) = A\prod_{k=1}^{q}\sqrt{(1 + x_k^2 + y_k^2 - 2x_k\cos\omega - 2y_k\sin\omega)}$$

$$/\prod_{i=1}^{p}\sqrt{(1 + s_i^2 + l_i^2 - 2s_i\cos\omega - 2l_i\sin\omega)} \quad , \tag{7}$$

$$\varphi_W(\omega) = \sum_{k=1}^{q}(\arctan[(x_k\sin\omega - y_k\cos\omega)/(1 - x_k\cos\omega - y_k\sin\omega)]$$

$$- \sum_{i=1}^{q}(\arctan[(s_i\sin\omega - l_i\cos\omega)/(1 - s_i\cos\omega - l_i\sin\omega)] \quad . \tag{8}$$

The causal characteristic and phase characteristic of wavelet are determined by pole-zeros location of the wavelet system function. Because symmetrical mapping pole-zeros method can change its causal characteristic and phase characteristic, a series of filters which have same amplitude spectrum and different causal characteristics and phase characteristics can be constructed. Substituting $C_k(z) = 1 - c_k z^{-1}$ of formula (2) for $C_k'(z) = |c_k|[1-(1/\bar{c}_k)z^{-1}]$, the zeros of the new system function and that of the real wavelet system function are symmetrical to $|z| = 1$ in the z-plane, that is the new system function maps $C_k(z)$ to $C_k'(z)$ symmetrically,

$$C_k'(e^{j\omega}) = |c_k|[1 - (1/\bar{c})e^{-j\omega}]$$

$$= [x_k^2 + y_k^2 - x\cos\omega - y\sin\omega]/\sqrt{(x_k^2 + y_k^2)}$$

$$+ j[x_k\sin\omega - y_k\cos\omega]/\sqrt{(x_k^2 + y_k^2)} \quad . \tag{9}$$

Its amplitude spectrum and phase spectrum are defined as,

$$C'_k(\omega) = \sqrt{[1 + x_k^2 + y_k^2 - 2x_k\cos\omega - 2y_k\sin\omega]} = C_k(\omega) \quad , \tag{10}$$

$$\varphi_{C'_k}(\omega) = \arctan[(x_k\sin\omega - y_k\cos\omega)/(x_k^2 + y_k^2 - x_k\cos\omega - y_k\sin\omega)] \quad . \tag{11}$$

From eqs. (5), (6), (10) and (11), when $C_k(z)$ is mapped to $C'_k(z)$ symmetrically, the amplitude spectrum of the wavelet is constant. When $|c_k| = 1$ (that is $x_k^2 + y_k^2 = 1$), $C_k(z)$ and $C'_k(z)$ are identical. In a similar way, when $D_i(z)$ is mapped to $D'_i(z) = |d_i|[1 - (1/\bar{d}_i)]z^{-1}$ symmetrically, it can also get the same conclusion. After mapping, the zeros of new system function and that of original system function are symmetrical on $|z| = 1$. So when one or more pole-zeros of filter system function are mapped on $|z| = 1$, a series of new system function with the same order, same amplitude spectrum and different phase spectra will be constructed, we can see them as estimated wavelets with the same amplitude spectrum and different phase spectrum. It should be noted that when the pole-zeros of wavelets are complex numbers, their conjugate complex roots must be mapped at the same time in order to ensure that the ARMA model's parameters are real. The roots on $|z| = 1$ unit circle don't need this process.

REFLECTION COEFFICIENT INVERSION

On the basis of constructing a series of wavelets with the same amplitude spectrum and different phase spectra, in order to research the effect of inaccurate wavelet phase estimation on reflection coefficient inversion, we need an appropriate inversion method. The existing inversion methods have been very mature, such as least squares deconvolution, minimum entropy deconvolution (Wiggins, 1978), sparse pulse deconvolution (Sacchi, 1997), multi-resolution signal deconvolution (Zhang and Li, 1999) and basis pursuit decomposition (Zhang and Castagna, 2011). Because of the wavelet described by ARMA model in time-domain is manifested as infinite impulse response sequence, time-domain deconvolution processing needs to cut the time-domain response inevitably. In order to reduce the effect of truncation error on inversion, we choose spectrum division to do the deconvolution in frequency-domain and map the frequency-domain results to the time-domain to compare.

Put the Robinson convolution model to Fourier transform,

$$X(e^{j\omega}) = W(e^{j\omega})R(e^{j\omega}) \quad , \tag{12}$$

where $X(e^{j\omega})$, $W(e^{j\omega})$ and $R(e^{j\omega})$ are frequency-domain representation of seismic record, wavelet and reflection coefficient sequences. The estimation of reflection coefficient sequences is,

$$\tilde{r}(n) = F^{-1}[\tilde{R}(e^{j\omega})] = F^{-1}[X(e^{j\omega})/\tilde{W}(e^{j\omega})] \quad , \tag{13}$$

where $\tilde{r}(n)$ is the time-domain estimation of reflection coefficient sequences, $\tilde{R}(e^{j\omega})$ is the frequency-domain estimation of reflection coefficient sequences, F^{-1} is the inverse Fourier transform operator, $\tilde{W}(e^{j\omega})$ is the frequency-domain representation of estimated wavelet.

Because of the estimated wavelet and real wavelet with the same amplitude spectrum, the convolution process is multiplication in the frequency-domain. Deconvolution process that gets rid of the influence of the wavelet is division in the frequency-domain. $W(e^{j\omega})$ and $\tilde{W}(e^{j\omega})$ have the same amplitude spectrum $W(\omega)$, their phase spectra are $\varphi_W(\omega)$ and $\varphi_{\tilde{W}}(\omega)$. According to the law of conservation of energy, the estimated reflection coefficient sequences $\tilde{r}(n)$ and the real reflection coefficient sequences $r(n)$ have the same energy. From eqs. (12) and (13),

$$\begin{aligned}\tilde{r}(n) &= F^{-1}[W(e^{j\omega})R(e^{j\omega})/\tilde{W}(e^{j\omega})] = F^{-1}[W(\omega)e^{j\varphi_W(\omega)}R(e^{j\omega})/\tilde{W}(\omega)e^{j\varphi_{\tilde{W}}(\omega)}] \\ &= F^{-1}[e^{j\varphi_W(\omega)-j\varphi_{\tilde{W}}(\omega)}R(e^{j\omega})] = F^{-1}(e^{j\varphi_W(\omega)-j\varphi_{\tilde{W}}(\omega)}) * r(n) \\ &= F^{-1}[P(e^{j\omega})] * r(n) = p(n) * r(n) \quad .\end{aligned} \tag{14}$$

Among them, $P(e^{j\omega}) = e^{j\varphi_W(\omega)-j\varphi_{\tilde{W}}(\omega)}$ is the frequency-domain representation of phase-only filter with unit energy, its all frequency components have unit amplitude. $p(n)$ is the time-domain sequence of phase-only filter. In theory, in the description of the ARMA model, the phase-only filters with any causal characteristic and phase characteristic can be constructed by the method described above.

From eq. (14), a phase-only filter can remain in the deconvolution results for the inaccurate wavelet phase estimation. The reflection coefficient inversion result is the convolution of reflection coefficient sequences and the phase-only filter, and the phase spectrum of the phase-only filter is the phase spectrum difference between the real and the estimated wavelet. The estimated reflection coefficient sequences and the original reflection coefficient sequences should have the same amplitude spectrum and energy, only the phase spectra have differences. Due to the influence of the phase-only filter, the estimated reflection coefficient sequences cause a phase offset which is not agreement with the distribution rule of original reflection coefficient sequences and is likely to cause illusions.

SIMULATION

In order to validate the influence of inaccurate wavelet phase estimation on reflection coefficient inversion in the description of ARMA model, this paper uses the sparse model with 4 pulses as the reflection coefficient sequences, whose length is 1000 ms, sampling frequency is 1 kHz, as shown in Fig. 1. The sparse pulses' location and size are (200 ms, 1.0), (300 ms, −0.8), (600 ms, 0.8), (800 ms, −1.0).

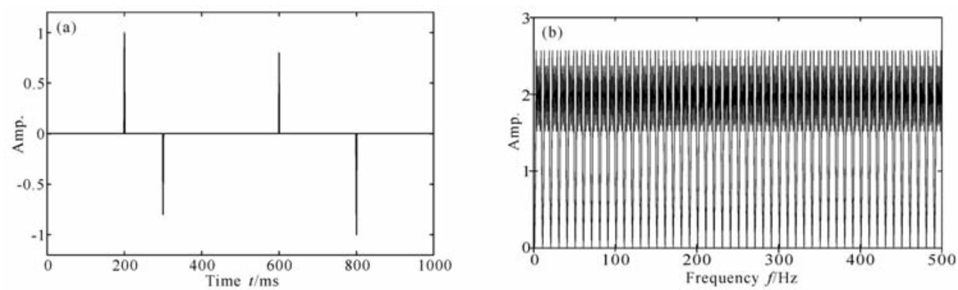

Fig. 1. The time domain waveform (a) and amplitude spectrum (b) of the reflection coefficient sequence model.

The causal mixed-phase wavelet is used in this experiment, the difference expression in the ARMA model is,

$$x(t) - 2.35x(t-1) + 2.12x(t-2) - 0.95x(t-3) + 0.21x(t-4)$$
$$= r(t) - 0.8r(t-1) + 0.2r(t-2) - 0.82r(t-3) \quad . \tag{15}$$

Its system function in the z-domain is,

$$W(z) = (1 - 0.8z^{-1} + 0.2z^{-2} - 0.82z^{-3})$$
$$/(1 - 2.35z^{-1} + 2.12z_{-2} - 0.95z^{-3}) + 0.21z^{-4}) \quad . \tag{16}$$

Calculating the roots of AR and MA part in eq. (16) can get the following results: True wavelet's poles are: $\alpha_1 = 0.8643 + 0.1666j$, $\alpha_2 = 0.8643 - 0.1666j$, $\alpha_3 = 0.3107 + 0.4177j$, $\alpha_4 = 0.3107 - 0.4177j$; and true wavelet's zeros are: $\beta_1 = 1.2015$, $\beta_2 = -0.2008 + 0.8013j$, $\beta_3 = -0.2008 - 0.8013j$. The time-domain and frequency-domain representation of the true wavelet is shown in Fig. 2, its time-domain waveform is interceptive. In this paper, the phase angle is $\varphi \in (-\pi,\pi)$ in the phase spectrum.

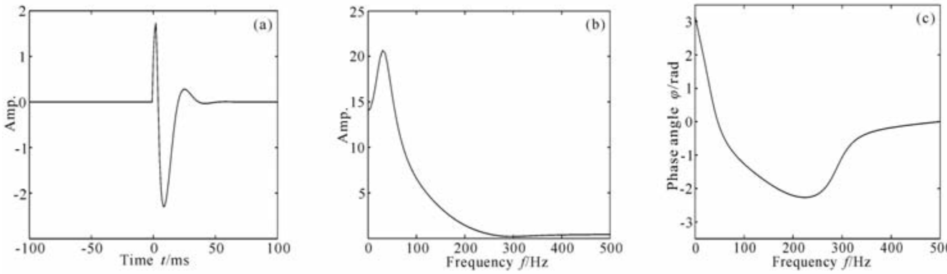

Fig. 2. The time domain waveform (a), amplitude spectrum (b) and phase spectrum(c) of the real wavelet.

The seismogram is synthesized by the convolution of the real wavelet and reflection coefficient sequence, the synthetic seismogram is shown in Fig. 3. Because of the wavelet described by the ARMA model, the synthetic seismogram has strong continuity in the time-domain, a long tail phenomenon is shown in Fig. 3(a). Contrasting Fig. 3(b) with Fig. 1, the energy of the synthetic seismogram is concentrated mostly in the low frequency region.

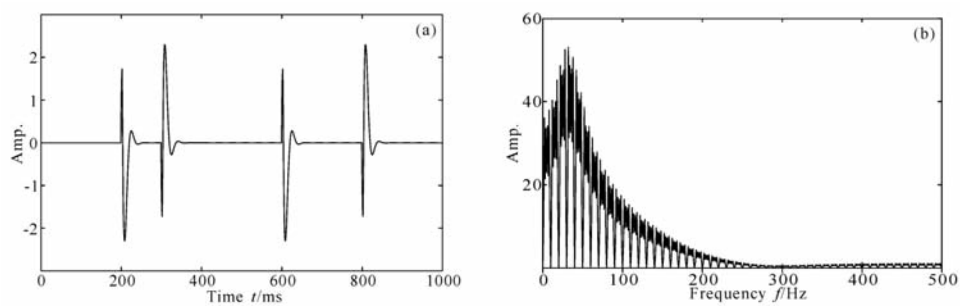

Fig. 3. The time domain waveform (a) and amplitude spectrum (b) of the synthetic seismogram.

A series of wavelets with the same amplitude spectrum and different phase spectrum are constructed by the method described in Section 2, their pole-zeros distribution in z-domain are shown in Fig. 4. In Fig. 4, "o" represents zero, "x" represents pole. The first line (4a-4d), the second and third line (4e-4l), the fourth line (4m-4p) are the pole-zeros distribution of the causal, the mix-causal, anti-causal wavelets. The first row, the second and third row, the fourth row are the pole-zeros distribution of the minimum-phase, the mixed-phase, maximum-phase wavelets. Fig. 4(b) is the pole-zeros distribution of true causal mixed-phase wavelet in the z-domain.

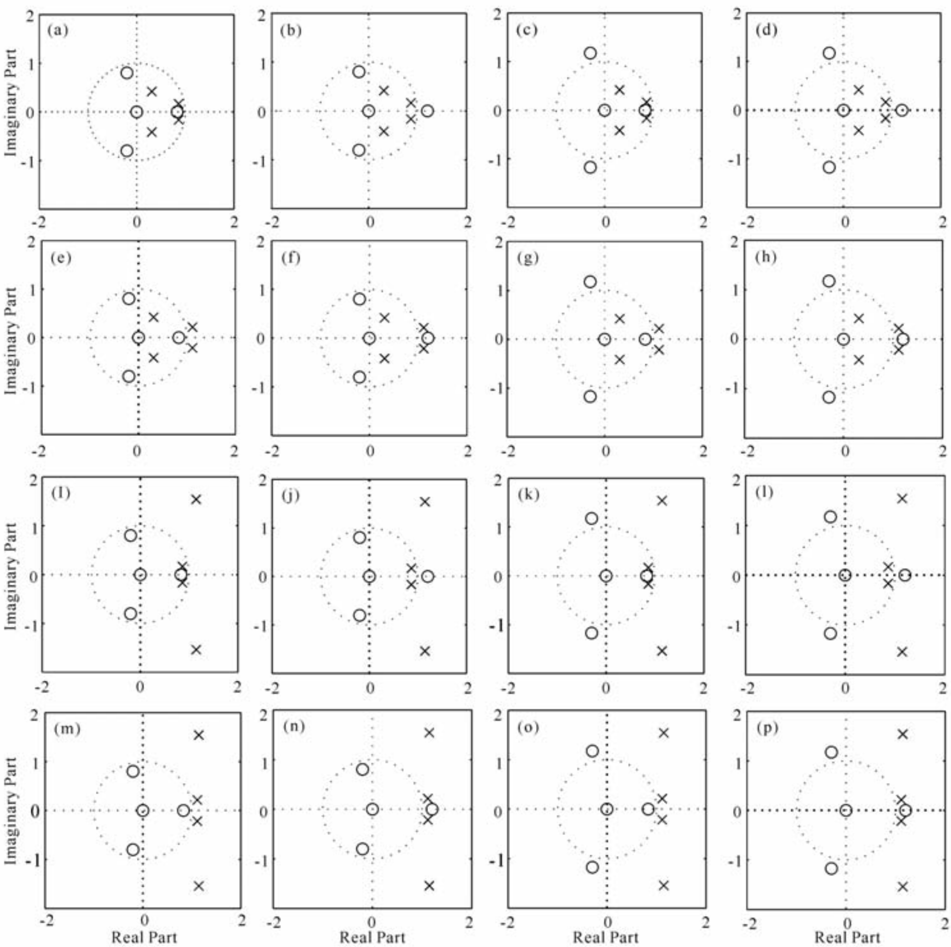

Fig. 4. Pole-Zeros of constructed seismic wavelets with different phase spectra.

The time-domain waveforms and phase spectra of wavelets with the same amplitude spectrum and different phase spectra are shown in Fig. 5. From Fig. 5, because of different phase spectra, the wavelets with the same amplitude spectrum have different characteristics in the time-domain. The waveforms in Fig. 5(b) have the corresponding phase spectra in Fig. 5(a), phase angle $\varphi \in (-\pi,\pi)$. From Fig. 5(a), No.1-4 wavelets are causal, all their time-domain response after the Time 0; No.5-12 wavelets are mix-causal, all their time-domain response before and after the Time 0; No.13-16 wavelets are anti-causal, all their time-domain response before the Time 0. No.2 is the original wavelet.

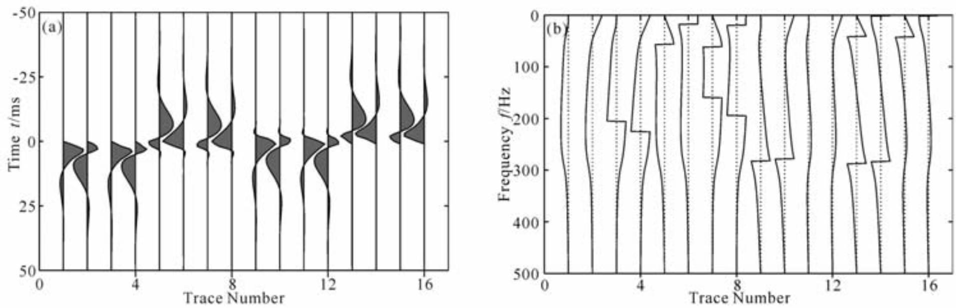

Fig. 5. The time domain waveform (a) and phase spectrum (b) of constructed seismic wavelets with the same amplitude spectrum and different phase spectra.

The constructed wavelets with the same amplitude spectrum and different phase spectra are used to implement reflection coefficient inversion for the synthetic seismogram, that is deconvolution. The deconvolution results of 16 wavelets are shown in Fig. 6. No.2 is the inversion result of the real wavelet.

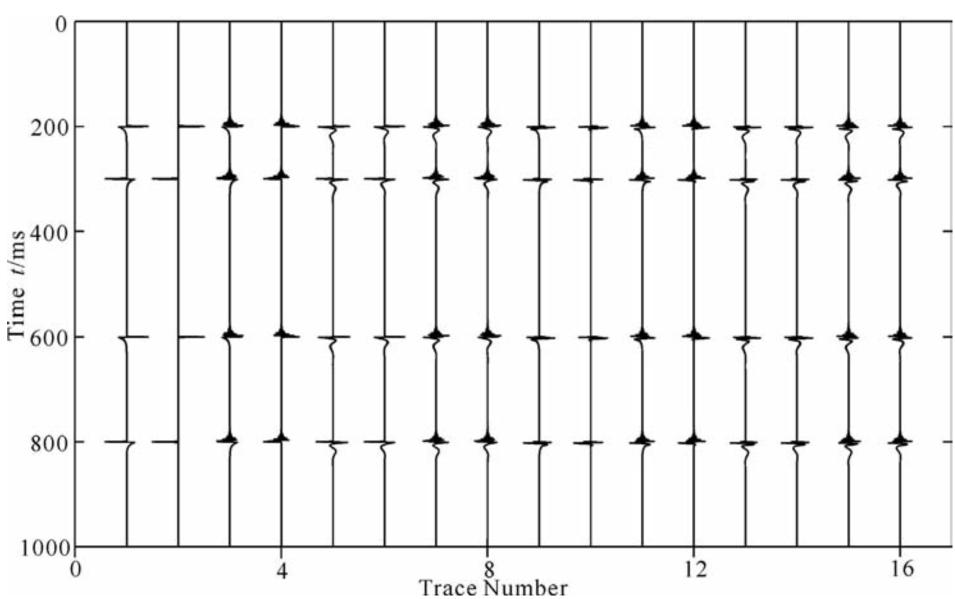

Fig. 6. The reflection coefficient inversion results of wavelets with different phase spectra.

From Fig. 6, only the real wavelet can restore the original reflection coefficient sequences completely, the inversion results of inaccurate phase wavelets are shown as the development form of the reflection coefficient in the time-domain and they do not meet the sparse properties of original reflection coefficient sequences. If the results meet the conclusions (below), the reflection coefficient inversion result is the convolution of original reflection coefficient sequences and a phase-only filter under the condition of inaccurate wavelet phase estimation, then all the reflection coefficient inversion results of estimated wavelets should have same amplitude spectrum (that is the same energy). According to the energy equivalence principle in the time-domain and the frequency-domain, calculating energy of all reflection coefficient inversion results in the time-domain and the frequency-domain, the results are shown in Table 1, No.2 is the inversion result energy of the real wavelet.

Table 1. The energy of reflection coefficient inversion results with different wavelets.

Trace Number	1	2	3	4	5	6	7	8
Time-domain Energy	3.2802	3.2800	3.2800	3.2802	3.2810	3.2808	3.2808	3.2810
Frequency-domain Energy	3.2802	3.2800	3.2800	3.2802	3.2810	3.2808	3.2808	3.2810
Trace Number	9	10	11	12	13	14	15	16
Time-domain Energy	3.2810	3.2808	3.2808	3.2810	3.2802	3.2800	3.2800	3.2802
Frequency-domain Energy	3.2810	3.2808	3.2808	3.2810	3.2802	3.2800	3.2800	3.2802

From Table 1, reflection coefficient inversion results of wavelets with different phase spectra have a slight energy difference, the root cause is that the ARMA model is infinite impulse response system. Because of the experimental reflection coefficient sequences with length of 1000 ms, it is cut off in the actual process then truncation error was produced. Numerical calculation also has accuracy error. But the maximum energy deviation of inversion results between estimated wavelets and real wavelet is less than 0.031% which belongs to the acceptable range. It can be considered that the reflection coefficient inversion results have the same energy and prove the Conclusions (below).

In order to further verify the Conclusions, phase-only filters will be calculated. From equation (14), phase-only filter can be obtained by,

$$P(e^{j\omega}) = e^{\,j\varphi_W(\omega)-j\varphi_{\tilde{W}}(\omega)} = W(e^{j\omega})/\tilde{W}(e^{j\omega}) \quad . \tag{17}$$

If some frequencies of the denominator in eq. (17) are equal to zero, they will be replaced by minimal real value in order to avoid a calculation error.

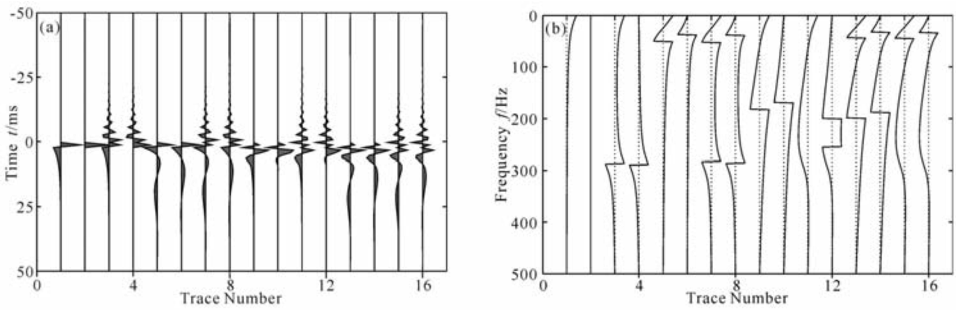

Fig. 7. The time domain waveform (a) and phase spectrum (b) of the phase-only filter.

Phase-only filters should have the same unit amplitude spectrum and the unit energy in the time-domain and the frequency-domain. Fig. 7 shows that the phase-only filters are calculated by eq. (17), the amplitude of each frequency in each filter is equal to 1, Fig. 7(a) are their time-domain waveforms, Fig. 7(b) are their phase spectra. Calculating the energy of 16 phase-only filters in the time- and the frequency-domain in Fig. 7, the results are shown in Table 2.

From Table 2 we can know that numerical calculation deviation and truncation error are less than 0.03% which belongs to the acceptable range. So we can consider that the obtained results have the same unit energy in time-domain and frequency-domain. Fig. 7 and Table 2 can prove that the results calculated by eq. (17) are phase-only filters.

Table 2. The energy of different phase-only filters.

Trace Number	1	2	3	4	5	6	7	8
Time-domain Energy	1.0001	1.0000	1.0000	1.0000	1.0003	1.0002	1.0002	1.0003
Frequency-domain Energy	1.0001	1.0000	1.0000	1.0001	1.0003	1.0002	1.0002	1.0003

Trace Number	9	10	11	12	13	14	15	16
Time-domain Energy	1.0003	1.0002	1.0002	1.0003	1.0001	1.0000	1.0000	1.0001
Frequency-domain Energy	1.0003	1.0002	1.0002	1.0003	1.0001	1.0000	1.0000	1.0001

Commanding the original reflection coefficient sequences to pass the phase-only filters, the results are shown in Fig. 8. We can see that the results in Fig. 6 are very similar to those in Fig. 8. In order to verify the results further, we can calculate the data similarity in Fig. 6 and Fig. 8 according to the same trace number, the results as shown in Table 3.

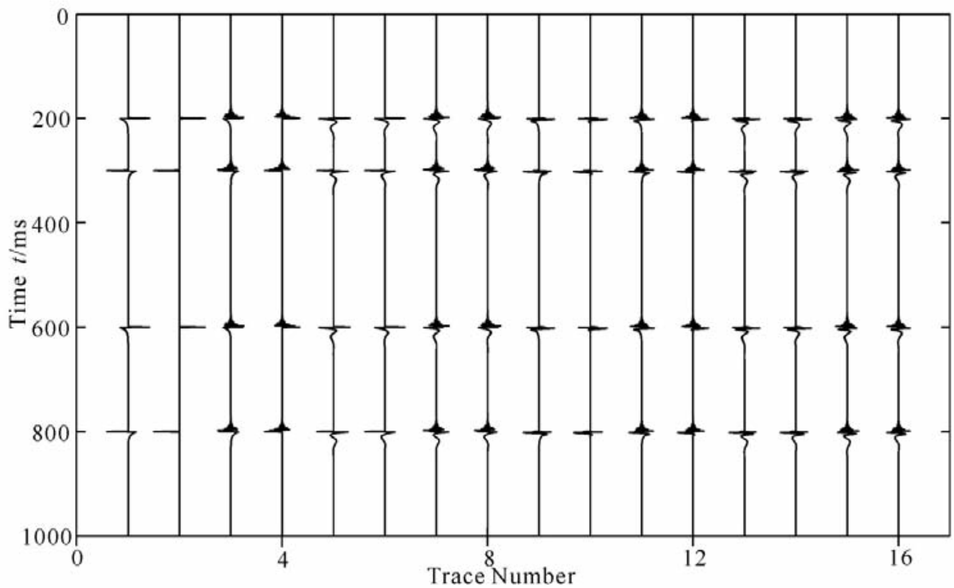

Fig. 8. The output of reflection coefficient sequences incentive different phase-only filters.

Table 3. Similarity between signal recovery results and phase-only filter results.

Trace Number	1	2	3	4	5	6	7	8
Similarity	100.00%	100.00%	99.99%	100.00%	100.00%	99.99%	100.00%	100.00%
Trace Number	9	10	11	12	13	14	15	16
Similarity	100.00%	100.00%	100.00%	100.00%	100.00%	100.00%	99.99%	99.99%

From Table 3, we can see that the results of reflection coefficient inversion and that of original reflection coefficient sequences passing phase-only filters have high similarity, the deviation of them can be seen as the numerical calculation deviation and truncation error. Then we can consider that reflection coefficient inversion result is the convolution of reflection coefficient sequences and a phase-only filter under the condition of inaccurate wavelet phase estimation.

In order to validate the phase spectrum of phase-only filter is the phase spectrum difference between real wavelet and estimated wavelet, we subtract phase spectrum of real wavelet to the estimated wavelet in Fig. 5, and the results are shown in Fig. 9.

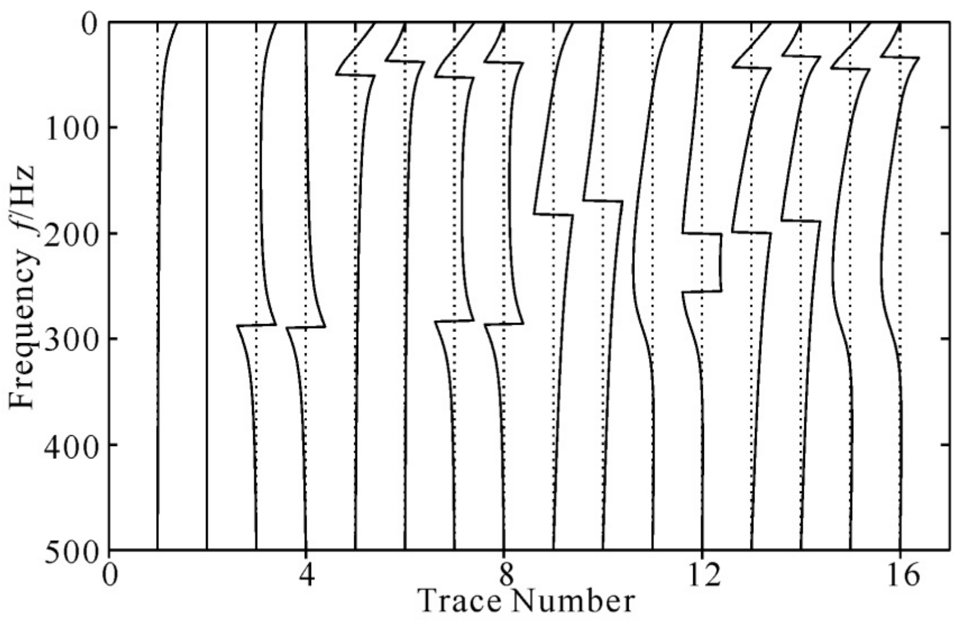

Fig. 9. The phase spectrum difference between real wavelet and estimated wavelets.

Contrasting Fig. 9 with Fig. 7(b), we can see that they are very similar. In order to validate the similarity of them, we can calculate the data similarity in Fig. 9 and Fig. 7(b) according to the same trace number, the results are shown in Table 4. Table 4 indicates that the phase-only filters' phase spectra and the phase spectra difference of real-estimated wavelets have high similarity. Then we can consider that the phase spectrum of phase-only filter is the phase spectrum difference between real wavelet and estimated wavelet.

Experimental results show that inaccurate wavelet phase estimation has effects on reflection coefficient inversion, the result of inversion is a convolution of original reflection coefficient sequences and a phase-only filter, and the phase spectrum of phase-only filter is the phase spectrum difference between real wavelet and estimated wavelet.

Table 4. Phase spectra similarity between phase-only filters and the difference of real-estimated wavelets.

Trace Number	1	2	3	4	5	6	7	8
Similarity	100.00%	100.00%	100.00%	100.00%	100.00%	100.00%	100.00%	100.00%
Trace Number	9	10	11	12	13	14	15	16
Similarity	100.00%	99.99%	100.00%	100.00%	100.00%	100.00%	100.00%	100.00%

RESULTS EVALUATION OF REFLECTION COEFFICIENT SEQUENCES

In actual seismic data processing, reflection coefficient sequences and real wavelet are both unknown. The amplitude spectrum of real wavelet is relatively easy to get, but the estimation of its phase spectrum is always not accurate. It can cause the phase deviation of reflection coefficient inversion results. Assuming that the original reflection coefficient sequences is sparse pulse sequence, its energy in time-domain focuses on several pulses. Although inversion results of inaccurate wavelet phase have the same energy, the energy will disperse in time-domain because phase spectra are changed. This paper will use the following evaluation methods to evaluate the inversion results and determine the real or accurate reflection coefficient sequences.

$$\Psi(\tilde{r})_1 = \sum_{i=0}^{L-1} |r_{i+1} - r_i| \quad , \tag{18}$$

$$\Psi(\tilde{r})_2 = \sum_{i=0}^{L} r_i^4 / (\sum_{k=0}^{L} r_k^2)^2 \quad . \tag{19}$$

Eqs. (18) and (19) which are called Variation and Kurtosis, respectively, are used to evaluate the reflection coefficient inversion results; these results are shown in Fig. 10.

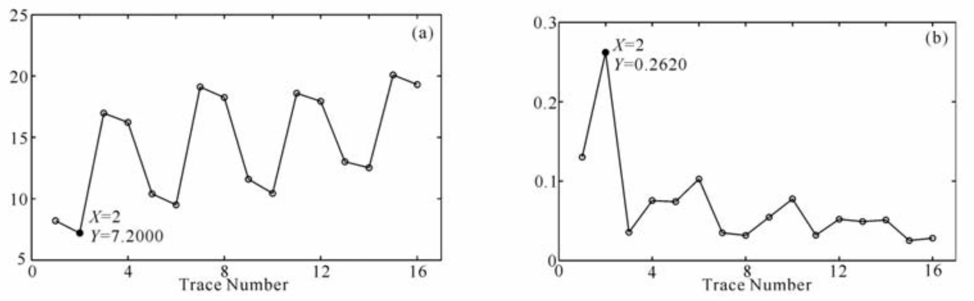

Fig.10 Evaluation results of reflection coefficient sequences with Variation (a) and Kurtosis (b).

Fig. 10 indicates that the minimum value of Variation is No.2; the maximum value of Kurtosis is No.2, too. It shows that Variation and Kurtosis can determine the accurate reflection coefficient sequences. Due to the real reflection coefficient sequences contained in the inversion results, the determined accurate reflection coefficient sequences are the real reflection coefficient sequences.

In order to validate the universality of above methods, assuming that the real wavelet is causal minimum-phase wavelet (No.1), mix-causal mix-phase wavelet (No.11), anti-causal maximum-phase wavelet (No.16); their reflection coefficient inversion results and evaluation results are shown in Fig. 11.

From Fig. 11, when the real wavelet is under the condition of any phase characteristic and causal characteristics, evaluation methods of Variation and Kurtosis can be used to evaluate the reflection coefficient inversion results and determine the real or accurate reflection coefficient sequences. In the same way, other evaluation methods of time-domain energy concentration can get the same results, so we will not reiterate them here.

ACTUAL SEISMIC DATA PROCESSING

In order to validate the influence rule of inaccurate wavelet phase estimation on reflection coefficient inversion, we will process the actual seismic data and reflection coefficient sequences in logging. Fig. 12(b) is seismic data in Shengli Oil Field, the digitization interval is 2 ms, and the well is near No.289 Trace. Fig. 12(a) is the reflection coefficient sequences in time-domain which converted from logging data.

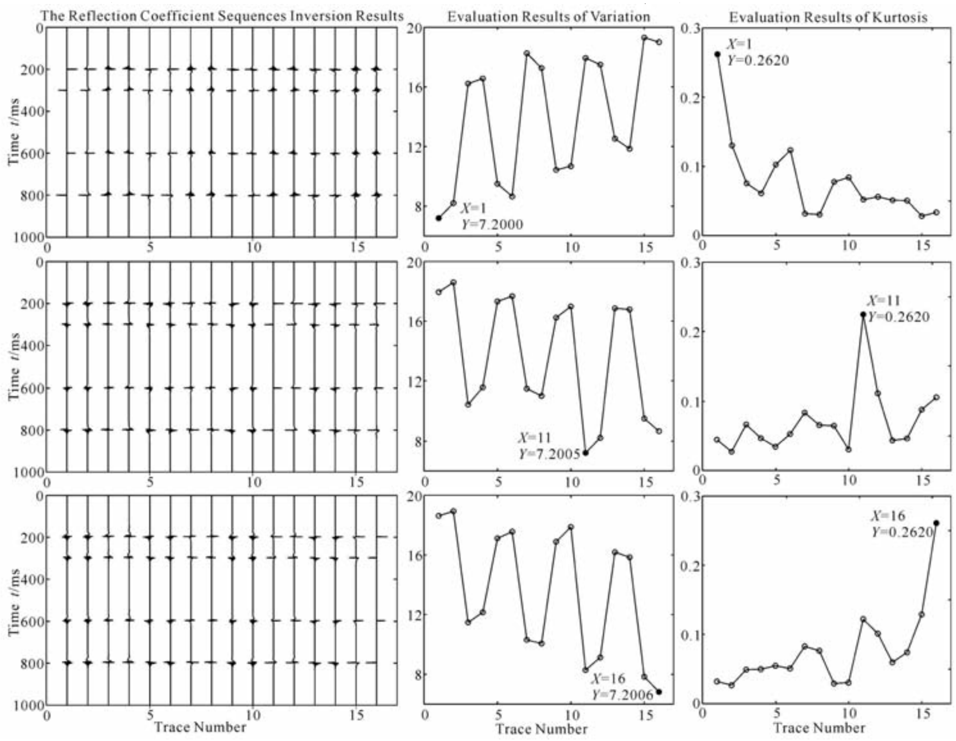

Fig. 11. Inversion and evaluation results of wavelets with different causal and phase characteristic.

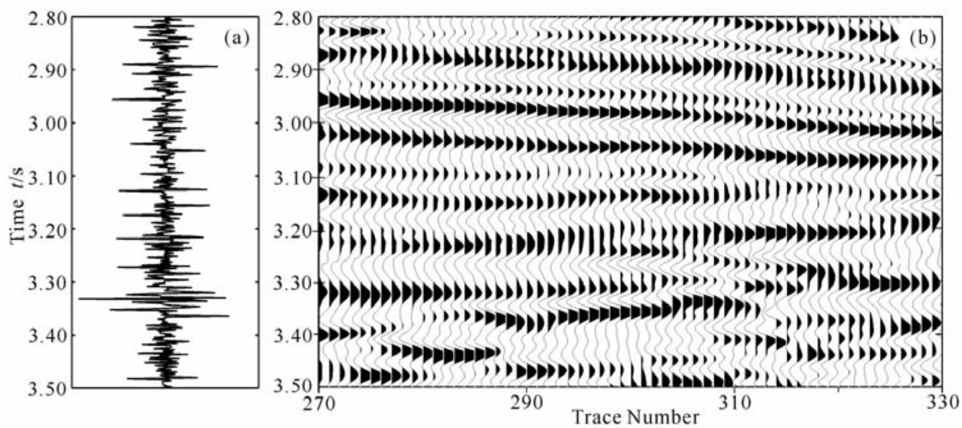

Fig. 12. Actual seismic data. (a) Reflection coefficient sequences of the 289th seismic trace, and (b) seismogram of the Shengli oil field.

The seismic wavelet was estimated in actual seismic data shown in Fig. 12. The uphole trace wavelet was extracted by the method of fine picking up seismic wavelet at uphole trace (Zhang and Liu, 2005), and the minimum-phase wavelet was estimated by traditional statistical seismic wavelet extraction method, both of them have the same amplitude spectrum. The results of seismic estimation are shown in Fig. 13.

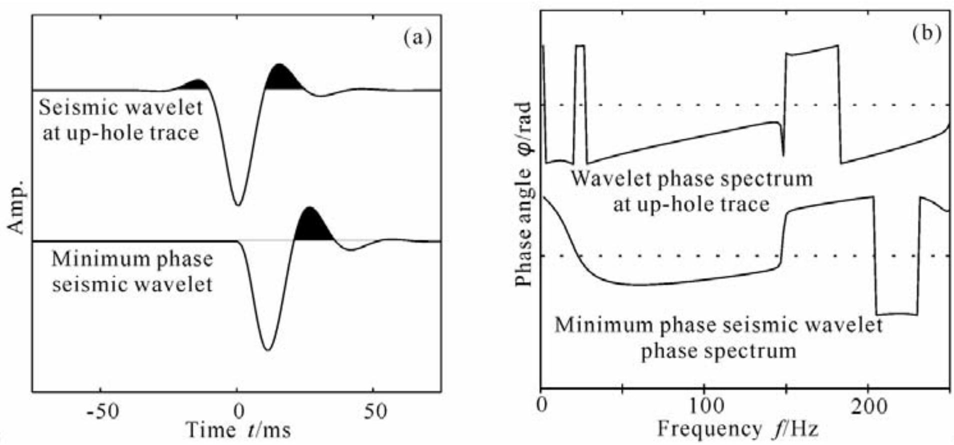

Fig. 13. Time domain waveforms (a) and phase spectra of wavelet estimation in actual seismic data.

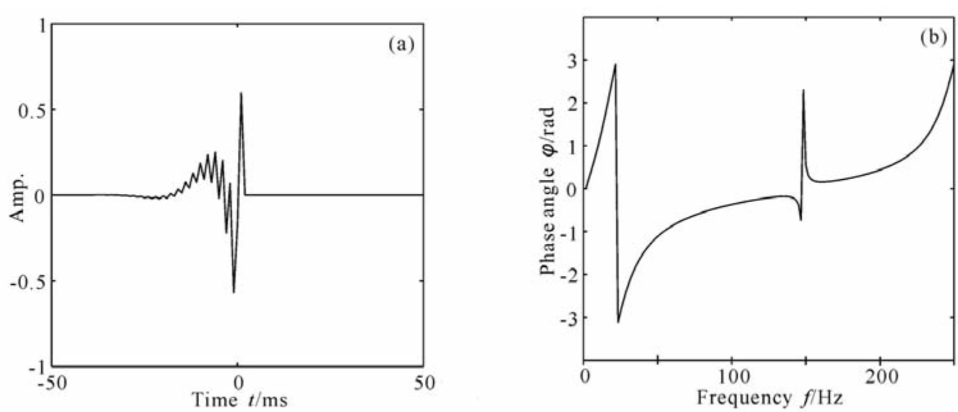

Fig. 14. The time domain waveform (a) and phase spectrum of constructed phase-only filter.

The uphole trace seismic wavelet is mix-causal mix-phase wavelet, and the seismic wavelet extracted by traditional method is causal minimum-phase as shown in Fig. 13. They have same amplitude spectrum and different spectra, in order to validate the effectiveness of the theory proposed by this paper, we make a subtraction between the two phase spectra so as to construct a phase-only filter. The constructed phase-only filter is shown in Fig. 14.

The reflection coefficient inversion was implemented by estimated minimum-phase wavelet for actual seismic data, and comparing the inversion results with the output of reflection coefficient sequences passing phase-only filter. The validity of proposed theory can be validated, if the results are consistent. The actual reflection coefficient sequences and inversion results are shown in Fig. 15.

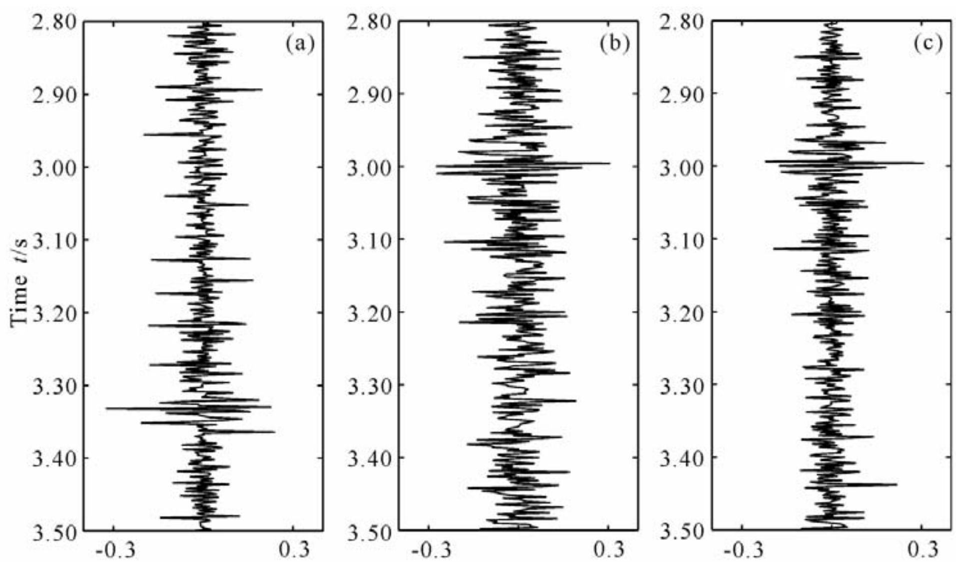

Fig. 15. Reflection coefficient sequences and inversion results. (a) Reflection coefficient sequences of logging, (b) minimum phase wavelet inversion results, and (c) phase-only filter results of reflection coefficient sequences.

Contrasting Fig. 15(a) with Fig. 15(b), in the condition of inaccurate seismic wavelet phase estimation, the inversion results which are greatly different from real reflection coefficient sequences can not reflect the formation of the actual stratigraphic information properly.[0] Because the estimated wavelet amplitude spectrum is accurate, the low-frequency component in seismic record was suppressed effectively after inversion. Contrasting Fig. 15(b) with

Fig. 15(c), the output of reflection coefficient sequences passing phase-only filter of Fig. 14 is similar to inversion results of minimum phase wavelet. They have high similarity with 73.74%. Considering the factors of seismic trace noise, time-depth conversion error and so on, the inversion results and reflection coefficient sequences calculation results have some error, but the similarity is in the acceptable range. The actual seismic data processing result can validate the conclusion that a phase-only filter can be remained in reflection coefficient inversion results for the inaccurate wavelet phase estimation, and the phase spectrum of phase-only filter is the phase spectrum difference between real wavelet and estimated wavelet.

Through the evaluation methods of Variation and Kurtosis, we can identify the real reflection coefficient sequences in Fig. 15 and verify the availability of evaluation methods[0]. The results of Variation and Kurtosis are shown in Table 5. * means the best result.

Table 5. Variation and Kurtosis evaluation results of actual seismic data.

	Reflection coefficient sequences of logging	Minimum phase wavelet inversion sesults	Results of reflection coefficient sequences passing phase-only filter
Evaluation results of Variation	25.2802*	38.0862	27.3185
Evaluation results of Kurtosis	0.0202*	0.0099	0.0154

CONCLUSIONS

This paper used the ARMA model to describe seismic wavelet, constructed the wavelets with the same amplitude spectrum and different phase spectra by the method of symmetric mapping pole-zeros of ARMA model in z-domain, and implemented reflection coefficient inversion to synthetic seismogram. The inversion results showed that reflection coefficient inversion result was a convolution of original reflection coefficient sequences and a phase-only filter when estimated wavelet and real wavelet with same amplitude spectrum and different phase spectra. The phase spectrum of phase-only filter is the phase spectrum difference between real wavelet and estimated wavelet. Due to the effect of phase-only filter, inversion results destroyed the sparseness of original reflection coefficient sequences (Energy concentration in time-domain). The inversion results were evaluated by two methods, the evaluation results showed that both the two methods can determine the real or accurate reflection coefficient sequences. In this paper, theoretical analysis, experimental simulation and actual seismic data processing were used to research the influence of inaccurate wavelet phase estimation on reflection coefficient inversion. The simulation and seismic data processing results can verify the theoretical analysis result. I hope this paper will give a research direction for improving the inversion results accuracy of reflection coefficient sequences.

ACKNOWLEDGEMENT

This work was supported by the National Natural Science Foundation of China (40974072), the Natural Science Foundation of Shandong Province (ZR2010DM14), the Fundamental Research Funds for the Central Universities (12CX06072A) and China University of Petroleum (East China) Graduate Student Innovation Project Funding (CX2013062).

REFERENCES

Cui, Q.H., Rui, Y.J. and Shang, X.M., 2011. Mixed-phase seismic wavelet extraction and its application. Geophys. Prosp. for Petrol., 50: 481-486.

Dai, Y.S., Wang, J.L. and Wang, W.W., 2008. Seismic wavelet extraction via cumulant-based ARMA model approach with linear and nonlinear combination. Chin. J. Geophys. (in Chinese), 51: 1851-1859.

Levy, S. and Oldenburg, D.W., 1982. The deconvolution of phase-shifted wavelets. Geophysics, 47: 1285-1294.

Levy, S. and Oldenburg, D.W., 1987. Automatic phase correction of common-midpoint stacked data. Geophysics, 52: 51-59.

Liang, G.H., 1998. On the methods of seismic wavelet extraction. Geophys. Prosp. for Petrol. (in Chinese), 37: 31-39.

Robinson, E.A., 1967. Predictive decomposition of time series with application to seismic exploration. Geophysics, 32: 418-484.

Sacchi, M.D., 1997. Re-weighting strategies in seismic deconvolution. Geophys. J. Internat., 12: 651-656.

Tang, B. and Yin, C., 2001. Non-minimum phase seismic wavelet reconstruction based on higher order statistics. Chin. J. Geophys. (in Chinese), 44: 404-410.

Wang, Y.H., 2003. A stable and efficient approach of inverse Q filtering. Geophysics, 67: 657-663.

Wang, Y.H., 2006. Inverse Q filter for seismic resolution enhancement. Geophysics, 71: 51-60.

Wiggins, R., 1978. Minimum entropy deconvolution. Geoexplor., 16: 21-35.

Wiggins, R., 1983. Entropy guided deconvolution. Geophysics, 50: 2720-2726.

Wu, Z.Y., 2004. Digital signal processing. Higher Education Press, Beijing.

Yi, Z.L. and Wang, R.Q., 2006. A new mixed phase deconvolution method. Oil Geophys. Prosp., 41: 266-270.

Yuan, S.Y. and Wang, S.X., 2010. Noise attenuation without spatial assumptions about seismic coherent events. Expanded Abstr, 80th Ann. Internat. SEG Mtg., Denver: 3524-3528.

Yuan, S.Y. and Wang, S.X., 2011. Influence of inaccurate wavelet phase estimation on seismic inversion. Appl. Geophys., 8: 48-59.

Zhang, G.Z., Liu, H. and Yin, X.Y., 2005. Method for fine picking up seismic wavelet at up-hole trace. Oil Geophys. Prosp., 40: 158-162.

Zhang, K., Li, Y.D. and Liu, G.Z., 1999. Multiresolution seismic signal deconvolution. Chin. J. Geophys. (in Chinese), 42: 529-535.

Zhang, R. and Castagna, J., 2011. Seismic sparse-layer reflectivity inversion using basis pursuit decomposition. Geophysics, 76: 147-158.